Available online at www.sciencedirect.com
ScienceDirect
Trans. Nonferrous Met. Soc. China 26(2016) 1670−1675
Transactions of Nonferrous Metals Society of China
www.tnmsc.cn

Luminescent properties of $Lu_2MoO_6:Eu^{3+}$ red phosphor for solid state lighting

Li LI[1], Jun SHEN[1], Xian-ju ZHOU[1], Yu PAN[1], Wen-xuan CHANG[1], Qi-wei HE[1], Xian-tao WEI[2]

1. College of Science, Chongqing University of Posts and Telecommunications, Chongqing 400065, China;
2. Department of Physics, University of Science and Technology of China, Hefei 230026, China

Received 14 July 2015; accepted 3 March 2016

Abstract: The Eu^{3+} activated Lu_2MoO_6 phosphors were synthesized by high-temperature solid-state reaction method. The X-ray diffraction (XRD), excitation spectra, emission spectra and decay lifetime of the phosphors were measured to characterize the structure and luminescent properties. The XRD results show that all the prepared phosphors can be assigned to the monoclinic structure. The experimental results indicate efficient absorption of near ultraviolet light from the Mo^{6+}–O^{2-} group followed by intensive emission in the visible spectral range. The optimal content of Eu^{3+} is 10% (mole fraction). The critical distance R_c and energy transfer mechanism were also discussed in detail. This red emitting material may be applied as a promising red phosphor for the near ultraviolet excited white light emitting diodes.

Key words: $Lu_2MoO_6:Eu^{3+}$; luminescent properties; red phosphor

1 Introduction

White light-emitting diodes (WLED) have recently attracted great attention as promising candidates for next-generation lighting due to its low energy consumption, high efficiency, excellent reliability, long lifetime, etc [1,2]. In order to generate white light using LEDs, one approach is to combine a blue LED chip emitting at 465 nm with a broad band yellow $Y_3Al_5O_{12}:Ce^{3+}$ ($YAG:Ce^{3+}$) phosphor. However, it exhibits low color rendering index (CRI) due to lacking of red component in the emission spectra, which limits its application. Another approach is to combine a near-ultraviolet (NUV) InGaN-based LED chip (350−420 nm) with the red, green and blue phosphors. In this approach, the phosphors are excited by the NUV chips, and the tricolor emissions make an excellent white light, which usually offer better color rendering performance [3]. Unfortunately, the efficiency of currently commercially used red phosphor $Y_2O_2S:Eu^{3+}$ is much lower than that of green and blue phosphors [4]. Therefore, more efforts should be devoted to searching for efficient red phosphors that can efficiently absorb light in the NUV region (350−420 nm).

Trivalent europium (Eu^{3+}) ions activated phosphors are considered as ideal red sources for WLED because of the sharp emission lines in the red spectral region [5]. For applications in NUV-based WLED, the phosphors should be able to efficiently absorb the emission from the LED chips. However, the *f*–*f* excitation of Eu^{3+} ions is narrow in bandwidth and weak in intensity due to the parity forbidden nature of the *f*–*f* transitions, which leads to the low efficiency. In order to enhance light absorption, sensitizers are introduced to absorb the excitation light and transfer the excitation energy to the Eu^{3+} ions, which is a feasible method to overcome this shortage and obtain promising red phosphors [6].

The Eu^{3+}-doped molybdates and tungstates were investigated because the MoO_4 and WO_4 groups can efficiently absorb ultraviolet light through the excitation of the Mo−O and W−O charge transfer states (CTS), respectively. This excitation is then followed by a transfer of the absorbed energy to Eu^{3+} ions for red emission [7,8]. Nevertheless, most of these materials exhibit low efficient absorption in the NUV region. Recently, much attention has been drawn to the Eu^{3+}-doped molybdate and tungstate R_2MO_6 (R=Y, Gd, La; M=Mo, W) for their remarkable properties such as excellent thermal and chemical stabilities and a broad

Foundation item: Project (11404047) supported by the National Natural Science Foundation of China; Projects (CSTC2015jcyjA50005, CSTC2014JCYJA50034) supported by the Natural Science Foundation Project of Chongqing, China; Project (KJ1500412, KJ1500409) supported by Scientific and Technological Research Program of Chongqing Municipal Education Commission, China
Corresponding author: Li LI; Tel: +86-23-62471721; E-mail: lilic@cqupt.edu.cn
DOI: 10.1016/S1003-6326(16)64276-0

excitation band [9−12]. However, little attention has been attracted to investigate the Eu^{3+}-doped Lu_2MoO_6 phosphors. LI et al [13] have synthesized the Lu_2MoO_6:Eu^{3+} phosphors by sol−gel method and investigated the structure and photoluminescence properties of such phosphors. However, the structural, luminescent properties and energy transfer mechanism of Eu^{3+}-doped Lu_2MoO_6 obtained by solid state reaction method were not studied. In this work, Eu^{3+}-doped Lu_2MoO_6 phosphors were synthesized using the high-temperature solid-state reaction method. The effect of Eu^{3+} molar concentration on the structure, luminescence and decay lifetime of the Lu_2MoO_6:Eu^{3+} phosphors was investigated. The energy transfer mechanism of Eu^{3+} in Lu_2MoO_6 host was also discussed in detail.

2 Experimental

2.1 Sample preparation

The Lu_2MoO_6:Eu^{3+} phosphors were synthesized by the high-temperature solid-state method. The starting materials are analytical reagent (AR) grade molybdenum trioxide (MoO_3), lutetium oxide (Lu_2O_3) (99.99%) and europium oxide (Eu_2O_3) (99.99%). The stoichiometric amounts of reactants were ground thoroughly in an agate mortar and preheated at 600 °C for 1 h. Subsequently, the products were removed from the muffle furnace, cooled, finely ground and sintered at 1200 °C for 4 h in air. Finally, the products were cooled to room temperature and then ground into white powder to form the final products.

2.2 Characterization

The crystal structures were analyzed by X-ray diffractometer (Persee, XD-2, Beijing Purkinje General Instrument Co., Ltd, Beijing, China) with Cu K_α radiation (λ=0.15406 nm). The excitation, emission spectra and the decay curves were measured by FLSP920 (Edinburgh Instrument Ltd, Livingston, UK) fluorescence spectrophotometer equipped with 450 W xenon lamp or a pulse xenon lamp as light sources and Shimidazu R9287 (Hamamatsu Photonics K.K., Hamamatsu, Japan) photomultiplier (200−900 nm) along with a liquid nitrogen-cooled InGaAs (Hamamatsu Photonics K.K.) (800−1700 nm) as the detectors. All spectra were collected at room temperature under identical experimental conditions so that the emission intensities of the samples with different Eu^{3+} doping concentrations can be compared.

3 Results and discussion

3.1 Structure analysis of Lu_2MoO_6:Eu^{3+} phosphors

Figure 1 shows unit cell of Lu_2MoO_6 drawn with VESTA [14]. This material is crystallized in the *I*2/*a* space group (No.15). The Lu^{3+} ions occupy three nonequivalent crystallographic sites, namely, 4e, 4e (with C_2 site symmetry) and 8f (with C_1 site symmetry), and all are coordinated to eight O atoms, whereas the Mo atoms are coordinated to five O atoms with four of which at a short distance and the other at a long distance [15].

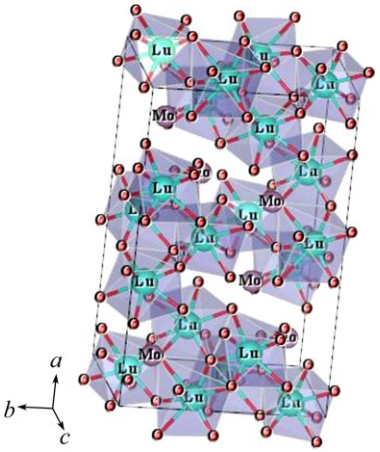

Fig. 1 One unit cell of Lu_2MoO_6 with 8-fold coordination of Lu^{3+} ions

Figure 2 shows the XRD patterns of Lu_2MoO_6 phosphors doped with $x$$Eu^{3+}$ (x=1%, 3%, 5%, 10%, 20%, 40%). It indicates that all the diffraction peaks coincide well with the data from the JCPDS card No. 25–0972 (Tm_2MoO_6), and Lu_2MoO_6 can be assigned to the monoclinic structure [13]. No additional peaks of other phases have been found, indicating that the Eu^{3+} ions are effectively doped into the host lattice. Additionally, the diffraction peaks of Lu_2MoO_6:Eu^{3+} samples are found to shift a little to lower angles with the increase of Eu^{3+} concentration, this is because the radius of Eu^{3+} (0.95 Å) is larger than that of Lu^{3+} (0.85 Å) in Lu_2MoO_6 host. When Lu^{3+} is substituted by Eu^{3+}, the interplanar distance *d* increases, the diffraction angles decrease according to

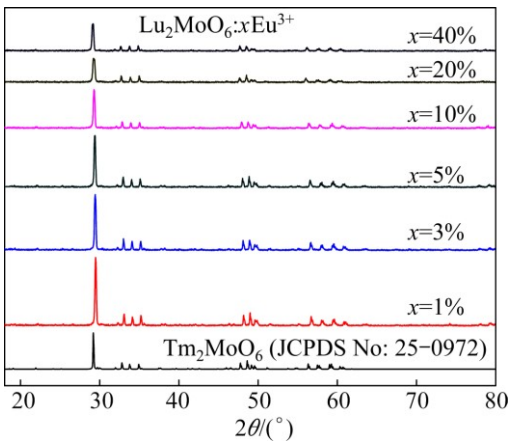

Fig. 2 X-ray diffraction patterns of Lu_2MoO_6:xEu^{3+} phosphor contrasted with standard pattern of JCPDS 25−0972

the Bragg equation: $2d\sin\theta=\lambda$, where d is the interplanar distance, θ is diffraction angle of peak, and λ is the X-ray wavelength (0.15405 nm). Therefore, it also demonstrates that Eu^{3+} ions are effectively doped into the Lu_2MoO_6 host to replace Lu^{3+} sites.

3.2 Photoluminescent properties and luminescence decay lifetime of Lu_2MoO_6:Eu^{3+} phosphors

Figure 3 shows the emission spectra of Lu_2MoO_6:xEu^{3+} phosphors under 363 nm excitation as a function of the Eu^{3+} concentration. The emission spectra of the Lu_2MoO_6:x%Eu^{3+} phosphors with similar shape consist of sharp lines with wavelength from 550 to 720 nm. The dominant red emission centered at 610 nm is assigned to the $^5D_0\rightarrow{}^7F_2$ transition of Eu^{3+} ions, while other weak emission located at 578 nm, 585 nm, 657 nm and 706 nm are attributed to the following transitions: $^5D_0\rightarrow{}^7F_0$, $^5D_0\rightarrow{}^7F_1$, $^5D_0\rightarrow{}^7F_3$ and $^5D_0\rightarrow{}^7F_4$, respectively. It is well-known that Eu^{3+} is an excellent probe ion, because the $^5D_0\rightarrow{}^7F_2$ transition (electric dipole allowed) is very hypersensitive to the chemical environment, while the $^5D_0\rightarrow{}^7F_1$ transition (magnetic dipole allowed) is insensitive to the environment. According to the Judd−Ofelt theory, the magnetic dipole transition is allowed. The electric dipole transition is permitted when the Eu^{3+} occupies the crystallographic sites without inversion symmetry [16]. Consequently, when the Eu^{3+} ions occupy the inversion center sites, the $^5D_0\rightarrow{}^7F_1$ transition should be relatively strong, while the $^5D_0\rightarrow{}^7F_2$ transition is very weak. The above experimental results indicate that the Eu^{3+} mainly occupies the nonequivalent crystallographic sites (both the C_1 and C_2) without inversion symmetry in the Lu_2MoO_6 lattice, which is consistent with the reported crystal structure of Lu_2MoO_6.

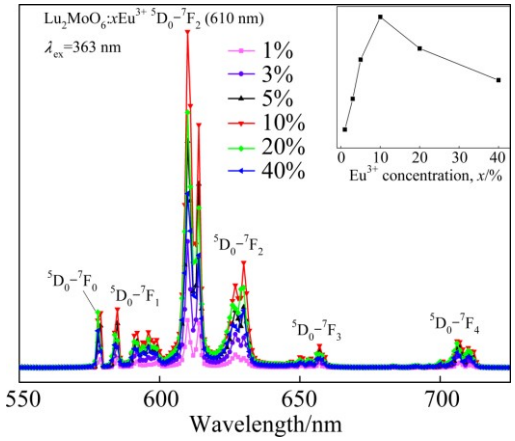

Fig. 3 Emission spectra of Lu_2MoO_6:xEu^{3+} phosphors (Inset represents emission intensity as function of Eu^{3+} concentration)

From the inset in Fig. 3, it is noticed that the emission intensity of 610 nm first increases and approaches a maximum at a doping concentration of 10% and then decreases with the increase of Eu^{3+} concentration. With the increase of Eu^{3+} concentration, the luminescence centers of Eu^{3+} increase, which results in increasing the emission intensity of Eu^{3+}. Whereas, when Eu^{3+} concentration is very high, the concentration quenching occurs, thus reducing emission intensity. The optimal doping concentration of Eu^{3+} is 10%.

In order to obtain the concentration quenching mechanism of Eu^{3+} under high doping concentration, the emission intensity of $^5D_0\rightarrow{}^7F_2$ transition (610 nm) is integrated under 363 nm according to the DEXTER theory [17,18], and its relationship with doping Eu^{3+} concentration (x) can be expressed as

$$I \propto x[1+\beta(x)^{s/3}]^{-1} \quad (2)$$

where s stands for the series of electronic multidipole interaction, s=3, 6, 8, 10 denote the exchange interactions of ions, dipole−dipole, dipole−quadrupole, quadrupole−quadrupole interactions, respectively, and β is a constant [19]. The value of s can be deduced from the slope $-s/3$ of the linear line in Fig. 4, which plots $\lg(I/x)$ vs $\lg x$ on a logarithmic scale of I/x. The slope $-s/3$ can be obtained as −2.1038 by fitting the data. Subsequently, the value of s is calculated as approximately 6. Thus, the results indicate that the concentration quenching mechanism of Eu^{3+} emission in the Lu_2MoO_6 host is attributed to the dipole−dipole interaction.

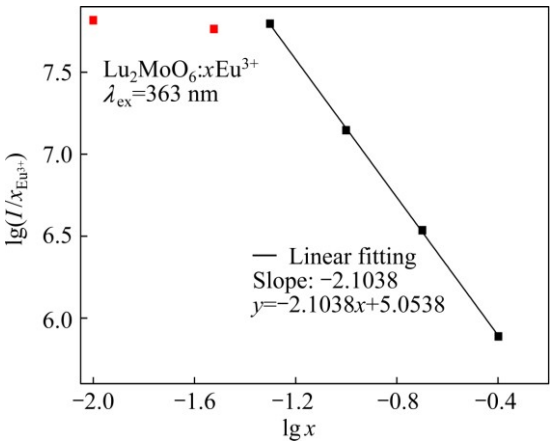

Fig. 4 Logarithmic plots for emission intensity per activator Eu^{3+} ion (I/x) as function of Eu^{3+} concentration (x) in Lu_2MoO_6:Eu^{3+} phosphors

Moreover, in terms of the Blasse's concentration quenching theory in inorganic phosphors [20], the critical distance R_c in Lu_2MoO_6:%Eu^{3+} phosphors can be estimated from the following equation:

$$R_c = 2\left(\frac{3V}{4\pi N x_c}\right)^{1/3} \quad (1)$$

where V is the volume of the unit cell of Lu_2MoO_6 (V=879.749 Å^3), x_c is the critical concentration of Eu^{3+} (x_c=0.1), and N is the number of host cations per unit cell (N=8) [13]. From Eq. (1), it can be calculated that the value of R_c is approximately equal to 12.8 Å. The results show the different values estimated from the other Eu^{3+}-doped phosphors [21,22], which emphasizes the influence of crystal structure on the luminescent properties of the Eu^{3+} ions. From the presented experimental results, it is seen that the Lu_2MoO_6:Eu^{3+} phosphors exhibit a strong red light with high color purity, which can be utilized to improve the color rendering property of white LEDs.

Figure 5 shows the excitation spectra of Lu_2MoO_6:xEu^{3+} phosphors monitoring the $^5D_0\rightarrow{}^7F_2$ emission at 610 nm. As shown in Fig. 5, the excitation spectra Lu_2MoO_6:xEu^{3+} phosphors all have the same profile, while the intensity declines with the increase of the Eu^{3+} concentration. The excitation spectra consist of two parts: the narrow excitation peaks between 450 nm and 550 nm and the intense broad band ranging from 250 nm to 440 nm. The broad band centered at 363 nm is attributed to the overlap of the Mo^{6+}−O^{2-} and Eu^{3+}−O^2 charge transfer states [23]. The narrow peaks at 462 nm and 530 nm correspond to the $^7F_0\rightarrow{}^5D_2$ and $^7F_0\rightarrow{}^5D_1$ transitions of Eu^{3+}, respectively. Therefore, the Lu_2MoO_6:Eu^{3+} phosphors can effectively absorb the emission in the 370−400 nm range from near-ultraviolet LED chips, which may be a potential candidate for application in near-ultraviolet excited WLED. Additionally, the observation of the Mo^{6+}−O^{2-} charge transfer state in the excitation spectra of Eu^{3+} indicates that energy transfer from the MoO_6^{6-} groups to the emitting Eu^{3+} ions is present.

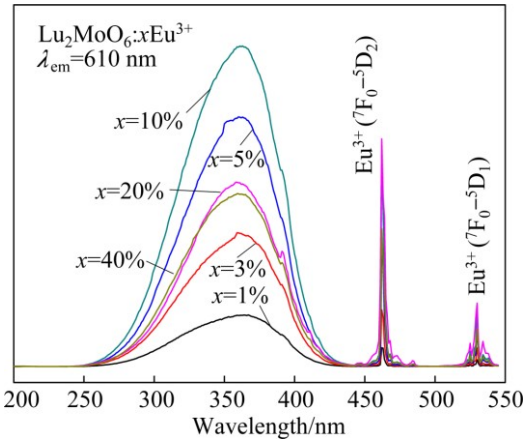

Fig. 5 Excitation spectra of Lu_2MoO_6:xEu^{3+} phosphors

Figure 6 shows the luminescence decay curves of red emission (610 nm) for Lu_2MoO_6:xEu^{3+} phosphors under 363 nm excitation. The decay curves of phosphors show nonexponential characteristics and a mean decay

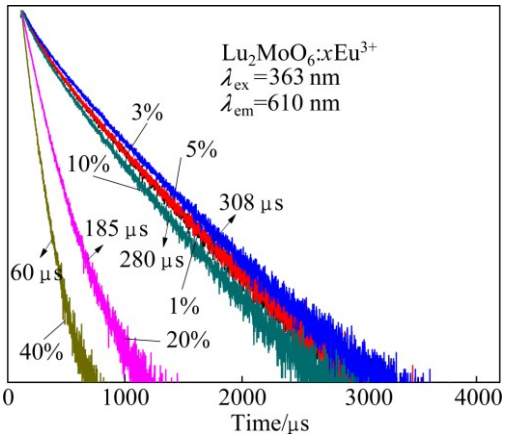

Fig. 6 Luminescence decay curves of Eu^{3+} (λ_{ex}=363 nm, λ_{em}=610 nm) in Lu_2MoO_6:xEu^{3+} phosphors

lifetime (τ_m) can be evaluated by

$$\tau_m = \int_0^t I(t)/I_0 \mathrm{d}t \quad (3)$$

where $I(t)$ is the luminescence intensity at the time t, and I_0 represents the initial intensity at t=0 [24]. The calculated lifetimes are shown in the inset in Fig. 6. When the concentration of Eu^{3+}(x) increases from 0 to 5%, there is no apparent change in the decay curve. As x reaches 10%, 20% and 40%, the faster decay was observed.

The emission spectra of the optimal Lu_2MoO_6: 10%Eu^{3+} and commercial Y_2O_2S:5%Eu^{3+} phosphors under 363 nm excitation are shown in Fig. 7. It is obvious that both the spectra show the characteristic emission of the Eu^{3+} ions. However, the spectral distributions are different as a result of different site symmetry for the Eu^{3+} ions in these two host lattices [5]. Moreover, the emission intensity of Lu_2MoO_6:10%Eu^{3+} under 363 nm excitation is about 2.2 times higher than that of Y_2O_2S:5%Eu^{3+} by comparing the two emission spectra. This result suggests that the Lu_2MoO_6:Eu^{3+} phosphors are potential red phosphors for near ultraviolet based solid state lighting.

Figure 8 shows the CIE (Commission Internationale de L'Eclairage) chromaticity diagram of Lu_2MoO_6: 10%Eu^{3+} phosphor under 363 nm excitation [25]. The Lu_2MoO_6:10%Eu^{3+} phosphors exhibit strong red emission. The corresponding chromaticity coordinates were calculated to be (0.65, 0.35), which are marked with Point 1 in the red luminescent region of Fig. 8. Expected values of the commercial Y_2O_2S:Eu^{3+} phosphors and the red phosphors are (0.62, 0.35) and (0.67, 0.33), which are shown with Points 2 and 3, respectively [26]. Based on our results, we suggest that Lu_2MoO_6:Eu^{3+} phosphors have met the commercial requirement in solid-state lighting.

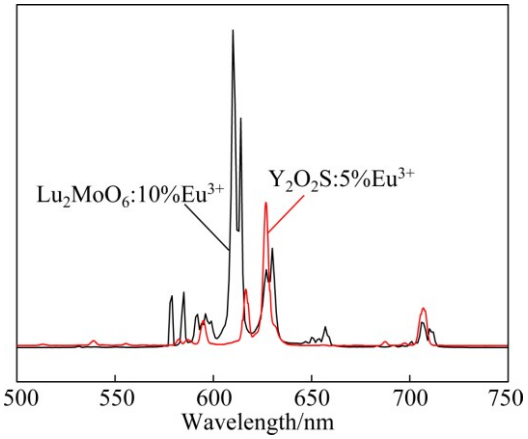

Fig. 7 Emission spectra of Lu_2MoO_6:10%Eu^{3+} and Y_2O_2S:5%Eu^{3+} phosphors under 363 nm excitation

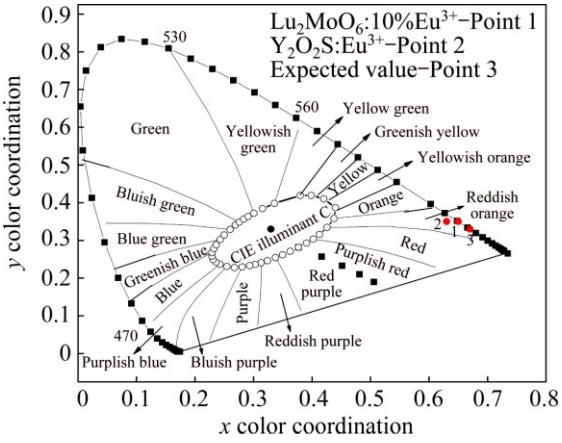

Fig. 8 CIE chromaticity diagrams of Lu_2MoO_6:10%Eu^{3+} phosphors under 363 nm excitation

3.3 Energy transfer mechanism

According to the investigation above, the energy level diagrams involved in the energy transfer process from the host to Eu^{3+} in Lu_2MoO_6 are presented in Fig. 9. Under ultra-violet light excitation, the MoO_6^{6-} group is excited owing to charge transfer transition from the O 2p states in the host's valence band to the Mo 4d states in the host's conduction band. The absorption energy can be transferred to the Eu^{3+} ions followed by red emission from the $^5D_0 \rightarrow {}^7F_J$ transitions as shown in Fig. 3, because the resonant nonradiative energy transfer will occur, as illustrated in Fig. 9.

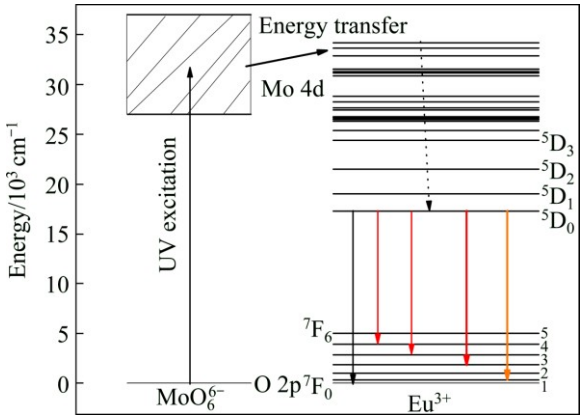

Fig. 9 Energy level diagram of MoO_6^{6-} and Eu^{3+} with energy transfer process

4 Conclusions

1) The Eu^{3+} activated Lu_2MoO_6 phosphors were synthesized by the high-temperature solid-state reaction method. The XRD results indicate that Lu_2MoO_6 can be assigned to the monoclinic structure.

2) The excitation and emission spectra show that Lu_2MoO_6:Eu^{3+} phosphors can be effectively excited by the near ultraviolet light (363 nm) and exhibit a strong red emission at 610 nm. The optimal Eu^{3+}-doped concentration and critical distance are 10% and 12.8 Å, respectively. The concentration quenching mechanism of Eu^{3+} emission in the Lu_2MoO_6 host is ascribed to the dipole−dipole interaction.

3) The experimental spectroscopic results presented in this work show the Lu_2MoO_6:Eu^{3+} phosphor as an excellent candidate for getting red emission for near ultraviolet based solid state lighting.

References

[1] LIN C C, LIU R S. Advances in phosphors for light-emitting diodes [J]. Journal of Physical Chemistry Letters, 2011, 2: 1268−1277.

[2] YE S, XIAO F, PAN Y X, MA Y Y, ZHANG Q Y. Phosphors in phosphor-converted white light-emitting diodes: Recent advances in materials, techniques and properties [J]. Materials Science and Engineering R, 2010, 71: 1−34.

[3] LIU R S, LIU YH, BAGKAR N C, HU S F. Enhanced luminescence of $SrSi_2O_2N_2$:Eu^{2+} phosphors by codoping with Ce^{3+}, Mn^{2+}, and Dy^{3+} ions [J]. Applied Physics Letters, 2007, 91: 061119.

[4] KUTTY T R N, NAG A. Role of interface states associated with transitional nanophase precipitates in the photoluminescence enhancement of $SrTiO_3$:Pr^{3+}, Al^{3+} [J]. Journal of Materials Chemistry, 2003,13: 2271−2278.

[5] DENG K M, GONG T, CHEN Y H, DUAN CK, YIN M. Efficient red-emitting phosphor for near-ultraviolet-based solid-state lighting [J]. Optics Letters, 2011, 36: 4470−4472.

[6] HAN B, ZHANG J, WANG Z M, LIU YY, SHI H Z. Investigation on the concentration quenching and energy transfer of red-light-emitting phosphor Y_2MoO_6:Eu^{3+} [J]. Journal of Luminescence, 2014, 149: 150−154.

[7] ZHOU L Y, WEI J S, YI L H, GONG F Z, HUANG J L, WANG W. A promising red phosphor $MgMoO_4$:Eu^{3+} for white light emitting diodes [J]. Materials Research Bulletin, 2009, 44: 1411−1414.

[8] WANG Z J, ZHONG J P, LIANG H B, WANG J. Luminescence properties of lutetium based redemitting phosphor $NaLu(WO_4)_2$:Eu^{3+} [J]. Optical Materials Express, 2013, 3: 418−425.

[9] WANG M F, ZHANG H, LI L, LIU X G, HONG F, LI R, SONG H J, GUI M X, SHEN J R, ZHU W H, WANG J B, ZHOU L Q, JEONG J H. Charge transfer bands of Mo−O and photoluminescence propertiesof micro-material Y_2MoO_6:Eu^{3+} red phosphor [J]. Journal of Alloys and Compounds, 2014, 585: 138−145.

[10] PANG M L, LIU X M. Luminescence properties of $R_2MoO_6:Eu^{3+}$ (R=Gd, Y, La) phosphors prepared by Pechini sol-gel process [J]. Journal of Materials Research, 2005, 20: 2676−2681.
[11] LI H Y, NOH H M, MOON B K, CHOI B C, JEONG J H, LEE H S, YI S S. Wide-band excited $Y_6(W Mo)_{0.5}O_{12}$:Eu red phosphor for white light emitting diode: Structure evolution, photoluminescence properties, and energy transfer mechanisms involved [J]. Inorganic Chemistry, 2013, 52: 11210−11217.
[12] LEI F, YAN B, CHEN H H. Solid-state synthesis, characterization and luminescent properties of Eu^{3+}-doped gadolinium tungstate and molybdate phosphors:$Gd_{(2-x)}MO_6:Eu_x^{3+}$ (M=W, Mo) [J]. Journal of Solid State Chemistry, 2008,181: 2845−2851.
[13] LI H Y, YANG H K, JEONG J H, JANG K, LEE H S, YI S S. Sol−gel synthesis, structure and photoluminescence properties of nanocrystalline Lu_2MoO_6:Eu [J]. Materials Research Bulletin, 2011, 46: 1352−1358.
[14] MOMMA K, IZUMI F. VESTA 3 for three-dimensional visualization of crystal, volumetric and morphology data [J]. Journal of Applied Crystallography, 2011, 44: 1272−1276.
[15] ALONSO J A, RIVILLAS F, MARTINEZ-LOPE M J, POMJAKUSHIN V. Preparation and structural study from neutron diffraction data of R_2MoO_6 (*R*=Dy, Ho, Er, Tm, Yb, Y) [J]. Journal of Solid State Chemistry, 2004, 177: 2470−2476.
[16] HAN B, LIANG H B, NI H Y, SU Q, YANG G T, SHI J Y, ZHANG G B. Intense red light emission of Eu^{3+} doped $LiGd(PO_3)_4$ for mercury-free lamps and plasma display panels application [J]. Optics Express, 2009, 17: 7138−7144.
[17] DEXTER D L. A theory of sensitized luminescence in solids [J]. Journal of Chemical Physics, 1953, 21: 836−850.
[18] DEXTER D L, JAMES H S. Theory of concentration quenching in inorganic phosphors [J]. Journal of Chemical Physics, 1954, 22: 1063−1070.
[19] van UITERT L G. Characterization of energy transfer interactions between rare earth ions [J]. Journal of the Electrochemical Society, 1967, 114: 1048−1053.
[20] BLASSE G. Energy transfer in oxidic phosphors [J]. Physics Letters A, 1968, 28: 444−445.
[21] YU R J, NOH H M, MOON B K, CHOI B C, JEONG J H, JANG K, YI S S, JANG J K. Synthesis and luminescence properties of a novel red-emitting phosphor $Ba_3La(PO_4)_3:Eu^{3+}$ for solid-state lighting [J]. Journal of Alloys and Compounds, 2013, 576: 236−241.
[22] GUO H, ZHANG H, WEI R F, ZHENG M D, ZHANG L H. Preparation, structural and luminescent properties of $Ba_2Gd_2Si_4O_{13}:Eu^{3+}$ for white LEDs [J]. Optics Express, 2011, 19: A201−A206.
[23] BLASSE G, CORSMIT A F. Electronic and vibrational spectra of ordered perovskites [J]. Journal of Solid State Chemistry, 1973, 6: 513−518.
[24] AN Y T, LABBE C, CARDIN J, MORALES M, GOURBILLEAU F. Highly efficient infrared quantum cutting in Tb^{3+}−Yb^{3+} codoped silicon oxynitride for solar cell applications [J]. Advanced Optical Materials, 2013, 1: 855−862.
[25] CHO H, HWANG S M, LEE J B, KA D H, KIM T W, LEE B S, LEE J Y, LEE J I, RYU J H. White luminescence of $Ho^{3+}/Tm^{3+}/Yb^{3+}$-codoped $CaWO_4$ synthesized via citrate complex route assisted by microwave irradiation[J]. Transactions of Nonferrous Metals Society of China, 2014, 24(S1): s134−s140.
[26] WANG Z J, LI P L, YANG Z P, GUO Q L. A novel red phosphor $BaZn_2(PO_4)_2:Sm^{3+}$, R^+ (R= Li, Na, K) [J]. Journal of Luminescence, 2012, 132: 1944−1948.

用于固态照明的红色荧光粉 $Lu_2MoO_6:Eu^{3+}$的发光性质

李 丽[1]，沈 君[1]，周贤菊[1]，潘 雨[1]，常文轩[1]，何琪伟[1]，韦先涛[2]

1. 重庆邮电大学 理学院，重庆 400065；
2. 中国科学技术大学 物理系，合肥 230026

摘 要：采用高温固相法制得 Eu^{3+}掺杂的 Lu_2MoO_6 荧光粉，通过 X 射线衍射(XRD)及激发、发射光谱和衰减寿命等手段对样品的结构和发光性质进行了表征。XRD 结果表明：制备的荧光粉均为单斜结构。实验结果表明该样品在可见光谱范围内能够被近紫外光有效地吸收，该吸收来自 Mo^{6+}–O^{2-}吸收带。在掺杂 10% Eu^{3+}的情况下，发光最强。详细地研究最佳临界距离 R_c 和能量机制。$Lu_2MoO_6:Eu^{3+}$ 红色荧光粉是一种可应用于近紫外激发白光 LED 用的新型红色荧光粉。

关键词：$Lu_2MoO_6:Eu^{3+}$；发光性质；红色荧光粉

(Edited by Yun-bin HE)